LAWRENCE
LIVERMORE
NATIONAL
LABORATORY

Characteristics of High Energy Ka and Bremsstrahlung Sources Generated by Short Pulse Petawatt Lasers

H.-S. Park, N. Izumi, M. H. Key, J. A. Koch, O. L. Landen, P. K. Patel, T. W. Phillips, B. B. Zhang

April 16, 2004

Disclaimer

Characteristics of High Energy Kα and Bremsstrahlung Sources Generated by Short Pulse Petawatt Lasers

H.-S. Park*, N. Izumi, M. H. Key, J. A. Koch, O. L. Landen, P. K. Patel, T. W. Phillips
University of California, Lawrence Livermore National Laboratory, Livermore, CA USA 94551
E-mail: park1@llnl.gov
B. B. Zhang
University of California, Davis, CA USA 95616

We have measured the characteristics of high energy Kα sources created with the Vulcan Petawatt laser at RAL and the JanUSP laser at LLNL. High energy x-ray backlighters will be essential for radiographing High-Energy-Density Experimental Science (HEDES) targets for NIF projects especially to probe implosions and high areal density planar samples. Hard Kα x-ray photons are created through relativistic electron plasma interactions in the target material after irradiation by short pulse high intensity lasers. For our Vulcan experiment, we employed a CsI scintillator/CCD camera for imaging and a CCD camera for single photon counting. We measured the Ag Kα source (22 keV) size using a pinhole array and the Kα flux using a single photon counting method. We also radiographed a high Z target using the high energy broadband x-rays generated from these short pulse lasers. This paper will present results from these experiments.

INTRODUCTION

X-ray radiography using backlighter sources has been an important tool for diagnosing and imaging various stages of planar and convergent hydrodynamics. Until now, hydrodynamics experiments at Omega utilize <9 keV backlighter x-rays emitted by thermal plasmas generated from a target material. However, the larger and denser NIF targets will need an x-ray probe with energies of 20 to 100 keV to study their hydrodynamics, atomic structure, equations-of-state, and other properties.

An efficient high-energy x-ray radiography source can be created using an ultra-high-intensity laser, which produces high-energy non-thermal x-rays from interactions between relativistic electrons and cold target atoms. These electrons produce Kα fluorescence emission in any mid-to-high Z solid, and these 20-100 keV x-rays can be used as semi-mono energetic backlighter sources for radiography. The construction of a multi-kJ, 1-10 ps Petawatt laser at NIF is planned to generate adequate 20-100 keV x-rays for high-energy x-ray radiography applications.

However, we have little understanding of the x-ray source parameters at the experimental conditions of interest. The x-ray conversion efficiency and source size are particularly important parameters needed to estimate the spatial resolution and signal level for a HEDES target. We began by characterizing the Ag Kα (22 keV) and Sm Kα (40 keV) sources generated by the the Vulcan Petawatt laser at RAL and the JanUSP laser at LLNL. For these experiments, the source was filtered by a Kedge filter to reduce high energy Bremsstrahlung background.

RAL EXPERIMENTAL SETUP

We performed the RAL experiment in Nov. 2003. The Vulcan laser at RAL can deliver up to 250 J of energy with 1 ps pulse duration into a > 8 μm diameter spot [Prav paper]. Figure 1 shows the experimental setup for this experiment. The laser hit the Ag target at ~20 degrees, and the reaction was
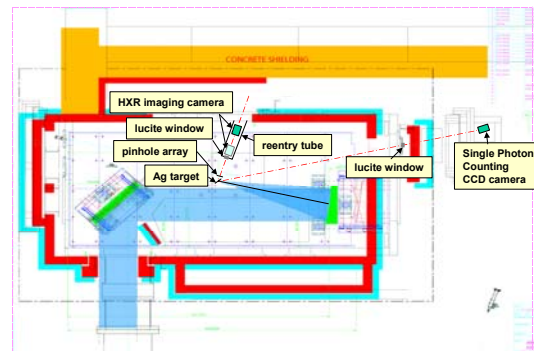

Fig 1. Experimental setup for the RAL petawatt experiment. A high energy x-ray imaging camera and a single photon counting camera were used.

monitored by two detectors. The first detector measured the x-ray spectrum using a single photon counting technique where a direct x-ray hit on a CCD produces electron-hole pairs that are proportional to the x-ray energy. The CCD is a 1300 x 1300 20 μm pixel CCD by EEV. This detector was placed 5.9 m away from the target center (TCC). The second detector imaged the Kα source size and shape using a pinhole array. The pinholes of 30 μm aperture were laser drilled on a 500 μm Ta substrate. The imaging detector is a CCD camera coupled to a CsI (Tl doped) scintillator custom made by LLNL [Ref Jason's paper]. Since we were interested in characterizing high energy x-rays, these detectors were placed outside the vacuum chamber and the target was viewed through a lucite window.

HIGH ENERGY Kα SOURCE SIZE

The 22 keV Ag Kα plus high energy Bremsstrahlung source filtered with a 50μm Ag foil was directly imaged using the pinhole array and the CsI/CCD camera. Fig 2 shows the pinhole image of this source and its measured FWHM. We performed similar measurements at Ag target thickness of 25, 50 and 100 μm and laser intensities of $10^{18} \sim 10^{20}$ W/cm^2. We find that the source size is independent
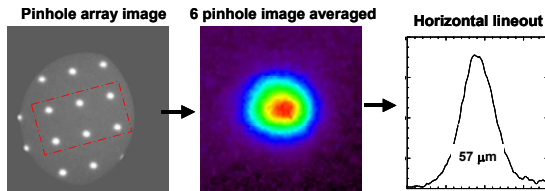
Fig 2. Pinhole image of 22 keV Ag Kα and high energy x-ray source generated by RAL petawatt laser.

of target thickness and laser intensity.

We also measured the source size for higher energy 40 keV Sm Kα radiation using the JanUSP laser at LLNL. Direct pinhole imaging was not possible because of the high energy background transmitted through the pinhole substrate (500 μm thick) dominated over the direct pinhole throughput. Instead we analyzed images of a 3 mm thick Ta knife-edge. Preliminary results show that the source size from the Sm target is also ~60 μm [Jason's paper.]

Our measured 60 μm x-ray source size is much bigger than the laser spot size (<10 μm) implying that the x-ray generated hot electrons produced by the laser are transported outside of the region of laser illumination. This spreading will limit the resolution

of point projection radiography schemes with this source.

Kα SOURCE CONVERSION EFFICIENCY

The conversion efficiency from laser energy to x-ray photon energy was measured by the single photon counting camera. Figure 3 shows an image from this camera taken during a laser shot. The first panel is the entire CCD and the second panel is a zoomed view of the central 100 x 100 pixel area. In the zoomed view, an x-ray hit is registered as a blob of connected pixels. Notice that the blobs are of different sizes and intensities, which result from the different x-ray photon energies.

For the analysis of this data we developed an algorithm that searches for the connected pixels, i.e. blobs, in these types of images and calculated the intensity of each blob. This algorithm first convolutes the pixilated image with a 2-dimensional Gaussian function that represents the best shape of the blobs. The Gaussian convolution works better

Entire CCD hit by X-ray photons	100x100 pxl zoomed view of central region
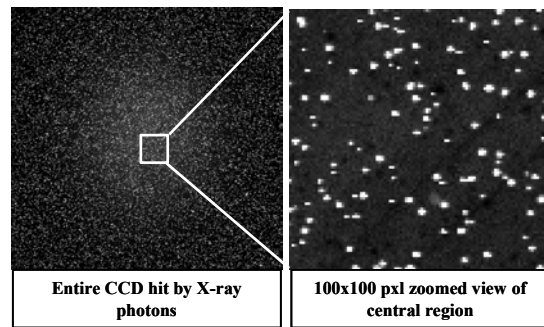
Fig 3. An image of x-ray hits from a laser interaction with an Ag target. The intensity of each blob is proportional to the x-ray energy.

than simply summing up the pixel values over a defined boxed region because the x-ray hits are too close to each other. The resulting histogram of the intensities is shown in Figure 4. For this shot, the laser energy was 192 J on the target and we defocused the laser to a 300 mm spot size with a 70
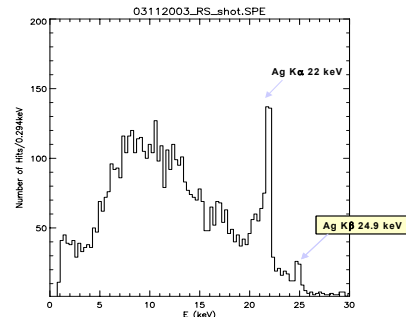
Fig 4. Histogram of single photon counting result.

ps pulse duration. The resulting intensity was 1.9 x 10^{17} W/cm^2. The lower intensity reduced the background. In this histogram the Kα and Kβ signals from the Ag target are clearly distinguishable.

From these histograms, we fit the backgrounds near the 22 keV peak with straight lines. The background subtracted histograma are then fit to Gaussian functions whose fitting parameters are used to calculate the integrated area of the peaks. This
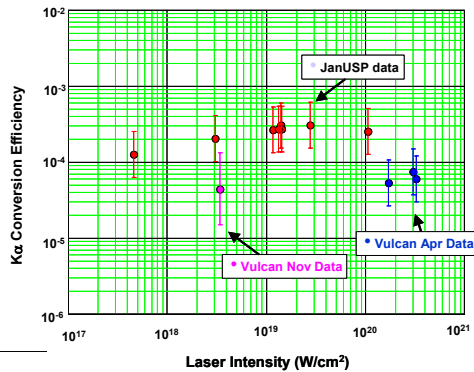

Fig 5. Measured laser energy to 22 keV Kα x-ray conversion efficiency (this plot needs to be redone)

integrated quantity represents the number of Kα x-rays observed in the data. This number is then corrected for the solid angle of the experimental set-up, the CCD 22 keV x-ray detection efficiency and the attenuation of the x-ray filters yielding the absolute total number of Kα photons generated in each laser shot. The conversion efficiency is the ratio of the total Kα energy to the total laser energy input. Figure 5 shows the resulting conversion efficiency as function of laser intensity from the different experiments.

22 keV Kα PRODUCTION FOIL THICKNESS DEPENDENCY

We measured the Ag Ka production efficiency as function of target foil thickness using the JanUSP laser. The laser energy was ~9.0 J with a 100 mm
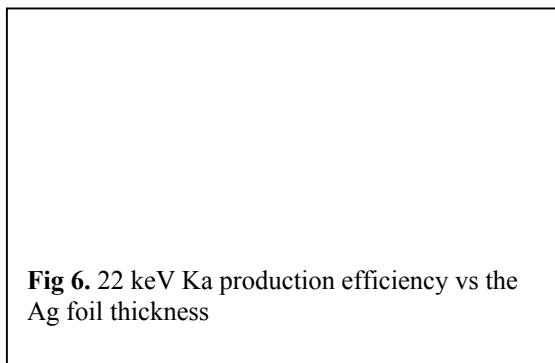
Fig 6. 22 keV Ka production efficiency vs the Ag foil thickness

spot size at a 5 ps pulse duration. The corresponding laser intensity was 1x 10^{19} W/cm^2. We maintained these laser parameters and shot Ag foils with thickness of 12.5, 25, 50, and 100 μm. The Ka production was measured by the single photon counting method described above. The result is shown in Fig. 6. We find that there is no change in Kα production over these ranges of Ag foil thickness. This could imply that the hot electron refluxing through the foil may be the dominating cause of Ka production or that the hot electrons are generated only on the surface of the foil.

CONCLUSION

We have directly measured the 22 keV Ag Kα source size using the RAL petawatt laser and performed knife-edge measurements of a 40 keV Sm Kα source using the JanUSP laser. The measured source sizes are both ~60 μm FWHM. These sources are not small enough to perform point projection radiography for NIF petawatt experiments since most experiments require better than 10 μm spatial resolution. We are now studying the option of using edge-on foil target geometries for high resolution 1-D imaging and different source shape geometries such as obtained from wire or microdot targets. We have also measured the Ag Kα conversion efficiencies. At laser intensities of 1x10^{18} W/cm^2 range, the conversion efficiency at 22 keV is ~ 1 x 10^{-5}. This number agrees to within a factor of 2 with a theoretical prediction that utilizes an analytic hot electron temperature distribution function and the ITS Monte Carlo. We are also developing a multilayer mirror for monochromatic imaging at 20~100 keV.

ACKNOWLEDGEMENT

REFERENCES

1. Z. Jiang *et al.*, Phys. Plasmas **2**, 1702 (1995).
J. Yu *et al.*, Phys. Plasmas **6**, 1318 (1999).
E. Andersson *et al.*, J. Appl. Phys. **90**, 3048 (2001).
K. Wharton, *et al.*, Phys. Rev. Lett. **81**, 822 (1998).
K. Yasuike, *et al.*, Rev. Sci. Instrum, **72**, 1236 (2001).
Ch. Reich *et al.*, Phys. Rev. Lett., **84**, 4846 (2000); Laser Part. Beams **19**, 147 (2001).